AGU PUBLICATIONS

JGR

Journal of Geophysical Research: Space Physics

RESEARCH ARTICLE

10.1002/2014JA020552

Key Points:
- A statistical analysis to the long-duration positive storm (LPS) effects over Jicamarca
- The occurrence of LPSs decays approximately exponentially after the main phase of the geomagnetic storms
- The disturbed electric field plays an essential role during the equatorial LPSs

Correspondence to:
L. Liu,
liul@mail.iggcas.ac.cn

Citation:
Kuai, J., L. Liu, J. Liu, B. Zhao, Y. Chen, H. Le, and W. Wan (2015), The long-duration positive storm effects in the equatorial ionosphere over Jicamarca, *J. Geophys. Res. Space Physics*, *120*, 1311–1324, doi:10.1002/2014JA020552.

Received 28 AUG 2014
Accepted 29 DEC 2014
Accepted article online 6 JAN 2015
Published online 3 FEB 2015

The long-duration positive storm effects in the equatorial ionosphere over Jicamarca

Jiawei Kuai[1,2,3], Libo Liu[1,2], Jing Liu[1,2], Biqiang Zhao[1,2], Yiding Chen[1,2], Huijun Le[1,2], and Weixing Wan[1,2]

[1]Key Laboratory of Earth and Planetary Physics, Institute of Geology and Geophysics, Chinese Academy of Sciences, Beijing, China, [2]Beijing National Observatory of Space Environment, Institute of Geology and Geophysics, Chinese Academy of Sciences, Beijing, China, [3]University of Chinese Academy of Sciences, Beijing, China

Abstract The long-duration positive storm (LPS) in the equatorial regions is relatively poorly understood. In this report, we conducted a statistical analysis of the LPS effects in the equatorial ionosphere over Jicamarca (12.0°S, 283.2°E) in 1998–2010. There are 250 geomagnetic storms (minimum $Dst < -50$ nT) in 1998–2010, but the ionosonde observations at Jicamarca are available only for 204 storms. A total of 46 LPSs are identified in terms of the criterion that the storm time relative deviation of peak density of F_2 layer (N_mF_2) exceeds 25% for more than 6 h. A salient feature is that the occurrence of LPSs tends to decay approximately exponentially on the following days after the main phase of geomagnetic storms. The ratios of the number of equatorial LPSs to that of geomagnetic storms have no obvious dependence on season and solar activity. During the daytime LPSs, the disturbed zonal electric field is mostly westward, as indicated from the geomagnetic field changes in the equatorial American region. For the nighttime LPSs, the significant uplifting of F_2 layer caused by an eastward electric field is the most important feature. Therefore, the disturbed electric field should play an essential role in forming the equatorial LPSs.

1. Introduction

During geomagnetic storms, the enhanced magnetospheric energy and energetic particles are deposited in the polar upper atmosphere and disturb the composition and dynamics of the whole thermosphere-ionosphere system. And ionospheric storms represent an extreme state of the ionosphere caused by geomagnetic storms. In the ionospheric F_2 region, these disturbances cause significant variations of electron density. The increase and decrease in ionospheric electron density are termed as positive and negative ionospheric storms, respectively. Observations and simulation results have revealed various features for these storm time ionospheric effects [e.g., *Prölss*, 1995; *Buonanto*, 1999; *Danilov and Lăstovička*, 2001; *Mendillo*, 2006; *Burns et al.*, 2007; *Danilov*, 2013]. For example, it is generally recognized that the occurrence and magnitude of the ionospheric storm effects are dependent on local time, latitude, season, and phase of the geomagnetic storm.

Up to now, the ionospheric negative storms are generally considered to be caused by the change in neutral compositions due to the heating of the thermosphere during geomagnetic storms. In contrast, the mechanisms of the ionospheric positive storms are still of controversy. A number of mechanisms have been proposed to explain the observed ionospheric features of positive storms [e.g., *Danilov and Belik*, 1992; *Prölss*, 1995; *Buonanto*, 1999; *Mendillo*, 2006; *Liu et al.*, 2010], such as the F_2 layer uplifting due to vertical drift induced by the equatorward neutral winds, the injection of plasma fluxes from the plasmasphere, and downwelling of the neutral species as a result of the storm time thermospheric circulation [*Danilov and Lăstovička*, 2001]. Especially, the altered thermospheric circulation causes downwelling of the neutral species through constant pressure surfaces at low middle latitudes, increasing the atomic O density relative to molecular N_2 and O_2 [e.g., *Liu et al.*, 2012b]. This change in O/N_2 produces increases in electron densities [*Fuller-Rowell et al.*, 1996].

At low latitude, the storm time-disturbed electric field is also an important factor that contributes to ionospheric storm effects. The storm-induced ionospheric disturbed electric fields redistribute the ionospheric plasma by creating positive/negative ionospheric storm and affect the occurrence of plasma density irregularities at low latitude and equatorial regions [e.g., *Fejer*, 1986; *Abdu*, 1997; *Sastri et al.*, 2000; *Bagiya et al.*, 2011]. The disturbed electric fields are broadly grouped into two categories: prompt penetration electric field (PPEF) and disturbance dynamo electric field (DDEF). Under the prompt penetration effect, the interplanetary electric

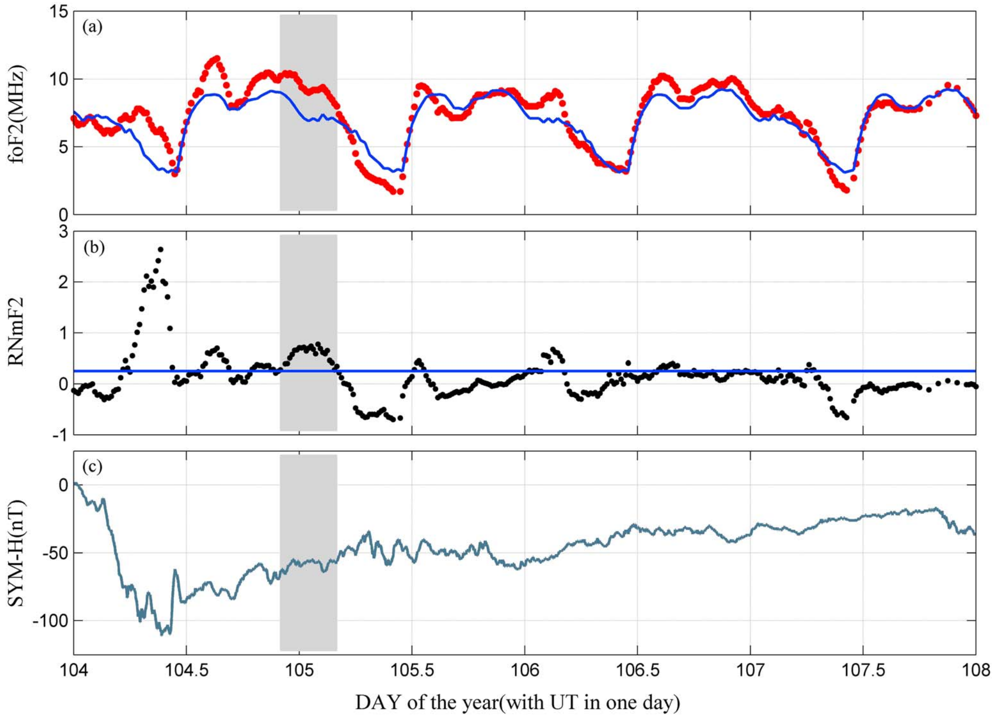

Figure 1. The schematic diagram of a long-duration positive storm (LPS) over Jicamarca during the geomagnetic storm that occurred on 14–17 April 2006. The figure gives the variations of (a) critical frequency of F_2 layer (f_oF_2), (b) relative deviation of N_mF_2 (RN_mF_2), and (c) *SYM-H* during the geomagnetic storm. The blue curves of Figure 1a denote the 27 day moving median value of f_oF_2. The blue curve in Figure 1b displays the reference value (0.25) of RN_mF_2 to judge a LPS. Using the criteria that RN_mF_2 exceeds 25% for more than 6 h, the gray shaded area indicates the period of this LPS.

field penetrates from high to low latitudes during geomagnetic storms. The PPEF is short lived and highly correlated with interplanetary magnetic field (IMF) *Bz* [e.g., *Fejer*, 1997; *Huang et al*., 2005b; *Wei et al*., 2011]. In general, on the dayside ionosphere, the southward turning of IMF B_z will result in eastward electric field disturbance, and a northward turning after prolonged southward IMF may lead to westward electric field disturbance. The DDEF arises from the ionospheric disturbance dynamo effects produced by the enhanced energy injection into the auroral region, which alters the global circulation and the generation of currents and electric fields. And the DDEF is westward on the dayside, i.e., opposite to the daytime ionospheric dynamo electric field and eastward on the nightside. Further, the DDEF is more slowly varying and is long lived even after magnetic activity and auroral heating have subsided [e.g., *Blanc and Richmond*, 1980; *Fejer et al*., 1983; *Sastri*, 1988; *Fejer*, 1997; *Bagiya et al*., 2011]. As a consequence, the composition changes, the storm time circulation wind, and the electrodynamics are all closely related to the ionospheric storm effects at low latitudes [*Liu et al*., 2004; *Bagiya et al*., 2014].

Among positive storms, the long-duration positive storm (LPS) is a special category event. The LPS could last over 6 h or even more than 12 h [*Pedatella et al*., 2009]. Many theories of positive storms were proposed to explain the LPSs. The downwelling of atomic O due to changes in thermospheric circulation and the uplifting of the F_2 layer due to the equatorward neutral winds during the storm time have been proposed for the formation of LPSs. In addition to equatorward winds, enhanced eastward electric fields can also lift the ionosphere to higher altitudes where the molecular recombination is less effective, and thus, the ionospheric *F* layer electron densities are increased [*Huang et al*., 2005a]. Another proposed mechanism for LPS is the exchange of plasma between the plasmasphere and ionosphere. The outer plasmasphere is convected away due to the enhanced magnetospheric electric fields and is refilled by ionospheric upflow during geomagnetic storms [*Lemaire and Gringauz*, 1998; *Schunk and Nagy*, 2000]. This causes a vertical redistribution of plasma, resulting in a decrease in the loss rate of electrons and then a relative increase in electron density. *Pedatella et al*. [2009] investigated the LPSs during the geomagnetic storm on 15 December 2006 using multiinstrument observations. They thought that refilling

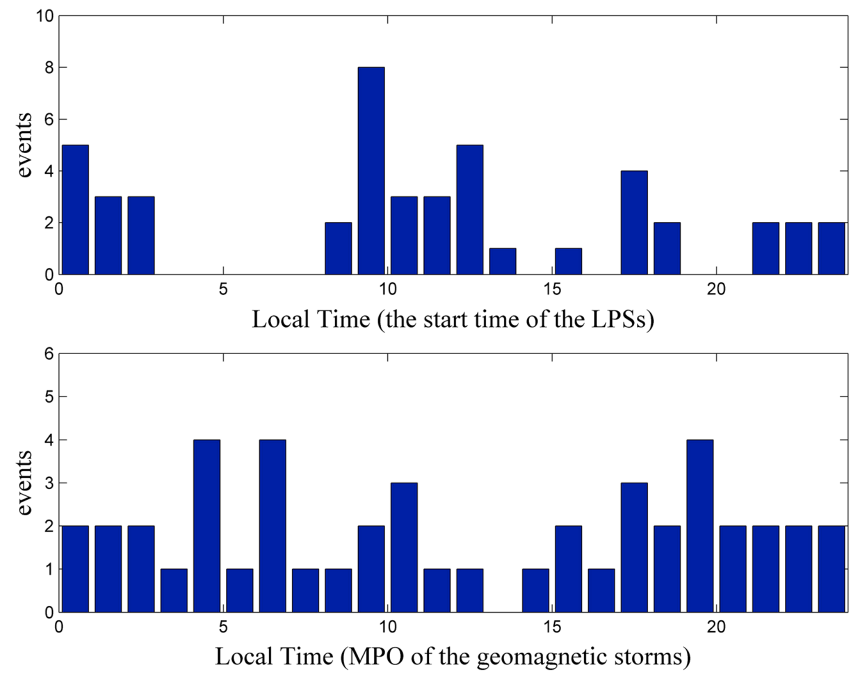

Figure 2. (top) The local time (LT) distribution of the observed long-duration positive storms (LPSs) at Jicamarca in 1998–2010 and (bottom) the LT distribution of the main phase onset (MPO) of the geomagnetic storms for all LPSs. In Figure 2 (top), the events counted for each local time are counted according to the start time of the LPSs.

of the topside ionosphere and plasmasphere is not the primary mechanism, but both the enhanced eastward electric field and equatorward neutral wind are likely to play a significant role in the generation of LPS effects. *Ngwira et al*. [2012] also observed a LPS over South Africa during the period of 24–27 July 2004. But this LPS is believed to be attributed to large-scale storm time thermospheric circulation. These observations reveal many features and mechanisms of the LPSs at low and middle latitudes.

Nevertheless, the occurrence and the mechanism of the LPSs in the equatorial regions are rarely understood, and relevant researches are also insufficient, which remain a challenge for the ionospheric community [*Prölss*, 1995; *Burns et al*., 2007]. In the present paper, we will conduct a statistical analysis to investigate the LPS effects in the equatorial regions using the ionosonde observations at Jicamarca (12.0°S, 283.2°E).

2. Data Presentation and Analysis

In this study, the ionograms recorded by a Digisonde Portable Sounder ionosonde at Jicamarca (12.0°S, 283.2°E) in 1998–2010 are collected for this analysis. We have manually edited the ionogram traces and used the SAO Explorer software package to retrieve the F_2 layer critical frequency (f_oF_2) and F_2 layer peak height (h_mF_2) based on the built-in true height inversion algorithm [*Huang and Reinisch*, 1996].

The daytime equatorial electrojet is a narrow band of enhanced eastward current flowing in the 100 to 120 km altitude region. The electrojet is caused by the equatorial electric field, and it can reflect the change of the electric field. In this work, because the measurement of the electric field in the equatorial regions is generally not available for statistics, the parameter *dH* is used to indicate the intensity of the electric field. The quantity $dH_{\text{JIC-PIU}}$ is used to present the difference in the magnitudes of the geomagnetic horizontal (*H*) component between Jicamarca and Piura (5.17°S, 80.64°W). The difference also provides a measurement of the daytime electrojet and the intensity of the $E \times B$ vertical drift in ionospheric *F* region [*Anderson et al*., 2002].

The data of the geomagnetic activity index (*Dst*) are obtained from the World Data Center for Geomagnetism, Kyoto (http://wdc.kugi.kyoto-u.ac.jp/dstdir/index.html). Solar wind parameters are downloaded from the Omni database [*King and Papitashvili*, 2005]. The symmetric component of ring current (*SYM-H*) can be regarded as a high-resolution version of the *Dst* index [*Wanliss and Showalter*, 2006]. And the *AE* index can roughly indicate the auroral energy inputs.

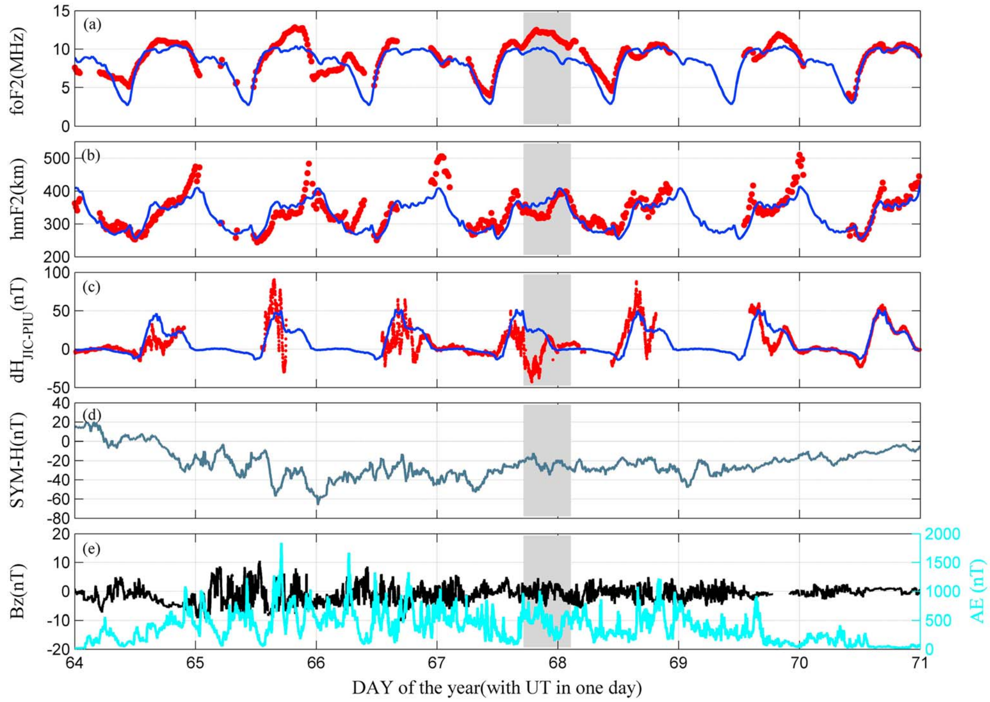

Figure 3. Variations of (a) critical frequency of F_2 layer (f_oF_2), (b) peak height of F_2 layer (h_mF_2), (c) $dH_{\mathrm{JIC\text{-}PIU}}$, (d) *SYM-H*, and (e) IMF B_z (gray line) and *AE* index (cyan line) during 5–11 March 2005. The blue curves of Figures 3a–3c denote the 27 day moving median value of these parameters. The $dH_{\mathrm{JIC\text{-}PIU}}$ is the difference in the magnitudes of the geomagnetic horizontal component between Jicamarca (12.0°S, 76.8°W, 0.8°N dip latitude) and Piura (5.17°S, 80.64°W, 6.8°N dip latitude), which provides a measure of the intensity of daytime ionospheric *F* region $E \times B$ vertical drift. The gray shaded area indicates the period of this daytime long-duration positive storm (LPS).

The data of [O]/[N_2] are obtained from the Global Ultraviolet Imager (GUVI), which is an instrument on board the Thermosphere-Ionosphere-Mesosphere Energetics and Dynamics (TIMED) satellite of NASA to investigate the far ultraviolet airglow of N_2, O_2, atomic oxygen, and other components from the upper atmosphere (http://guvi.jhuapl.edu/). In particular, the satellite samples almost the same local time in a few days. The daytime [O]/[N_2] column is calculated from OI 135.6 nm and N_2 Lyman-Brige-Hopfield dayglow brightness ratio in the nadir direction above the altitude where the N_2 column density is equal to 10^{17} cm^{-2} [*Strickland et al.*, 2004]. The [O]/[N_2] column can indicate the effects of the neutral composition changes.

The f_oF_2 is converted to the peak electric density N_mF_2 (=$1.24 \times (f_oF_2)^2 \times 10^4$ electrons/cm^3 with f_oF_2 in megahertz). The storm time relative deviation of N_mF_2 (RN_mF_2) is defined as follows:

$$RN_mF_2 = \frac{N_mF_2 - (N_mF_2)_Q}{(N_mF_2)_Q} \times 100\%$$

The parameter $(N_mF_2)_Q$ is the reference value of N_mF_2 during geomagnetically quiet conditions. There are many algorithms to calculate the reference value, such as the 27 day running median value, the monthly median value, and the seven quiet days running average [*Vijaya Lekshmi et al.*, 2011]. Each algorithm has its own characteristic. We choose a 27 day running median value as the reference $(N_mF_2)_Q$ in this work. The advantage of using running f_oF_2 median for F_2 layer disturbance analyses was stressed long ago [e.g., *Mednikova*, 1957]. A 27 day component is apparent in the solar EUV, due to the solar rotation, and in many ionospheric parameters [e.g., *Chen et al.*, 2012]. Therefore, the 27 day running smooth median is used mainly to remove the solar rotation effects. A geomagnetic storm is considered to produce an ionospheric storm if RN_mF_2 exceeds ±25% for more than 3 h, because the magnitude ±25% is set to represent the day-to-day variability of the ionosphere under quiet conditions [*Vijaya Lekshmi et al.*, 2011].

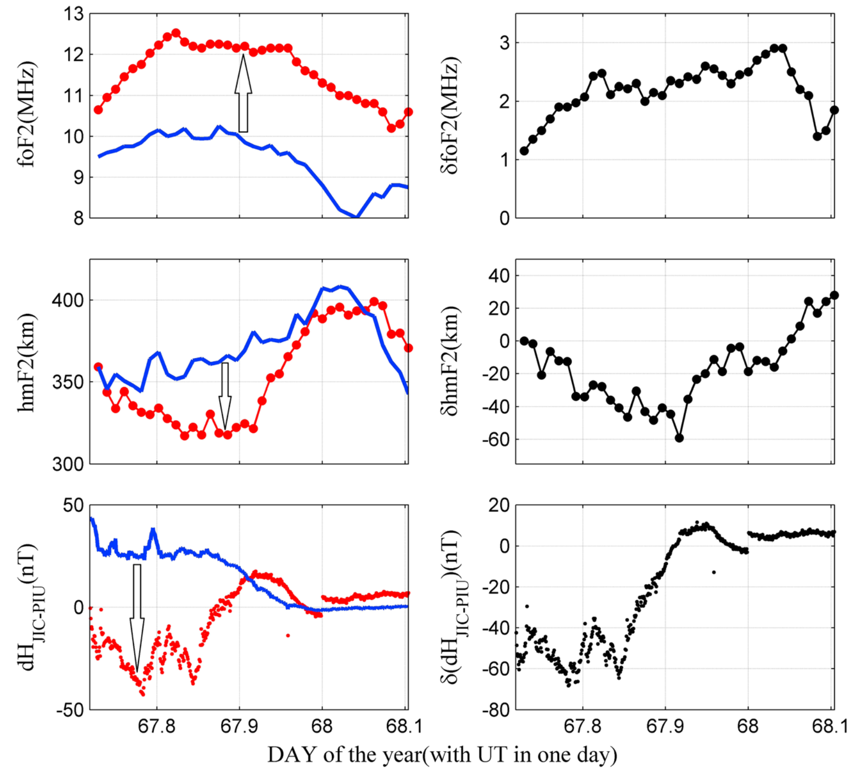

Figure 4. (left) The variations of (top) critical frequency of F_2 layer (f_oF_2), (middle) peak height of F_2 layer (h_mF_2), and (bottom) $dH_{\text{JIC-PIU}}$ during the long-duration positive storm (LPS) of 8–9 March 2005. The $dH_{\text{JIC-PIU}}$ is the difference in the magnitudes of the geomagnetic horizontal component between Jicamarca (12.0°S, 76.8°W, 0.8°N dip latitude) and Piura (5.17°S, 80.64°W, 6.8°N dip latitude), which provides a measure of the intensity of daytime ionospheric F region $E \times B$ vertical drift. The blue curves denote the 27 day moving median value of these parameters. (right) The deviation of these parameters on the left. There are good one-to-one correspondences among counter electrojet, decreased h_mF_2, and increased f_oF_2 in the equatorial ionosphere during the LPS.

We take a criterion to identify a LPS caused by a geomagnetic storm if RN_mF_2 exceeds 25% for more than 6 h. On one hand, the time scale of 6 h reflects the significant increase compared with 3 h of the general positive storms; on the other hand, the number of the LPSs with the time scale of 6 h has the statistical value because the number will be fewer if the time scale is more than 6 h. Figure 1 is the schematic diagram of a LPS over Jicamarca during the 14–17 April 2006 geomagnetic storm. The curve RN_mF_2 in Figure 1b reflects the criteria of the LPS.

3. Results

We conduct a statistical analysis on the LPSs during the geomagnetic storms that occurred in 1998–2010 over Jicamarca using the definition mentioned above. A total of 250 geomagnetic storms with the minimum $Dst < -50$ nT occurred during this period. However, the ionospheric data are only available for 204 storms at Jicamarca, and no data are available at Jicamarca for an interval in 2000–2001. In total, 46 LPSs are found over Jicamarca during the 204 available geomagnetic storms in 1998–2010. In particular, the number of LPS is counted only one time even though the LPS occurred more than one time during a geomagnetic storm.

3.1. Daytime LPS and Nighttime LPS

Figure 2 (top) gives the local time (LT) distribution of the observed LPSs at Jicamarca in 1998–2010, and Figure 2 (bottom) shows the LT distribution of the main phase onset (MPO) of the geomagnetic storms for all LPSs. In Figure 2 (top), the events counted for each local time are counted according to the start time of the LPSs. No LPS starts from 03:00 to 08:00 LT because of the prevailing appearance of

10.1002/2014JA020552

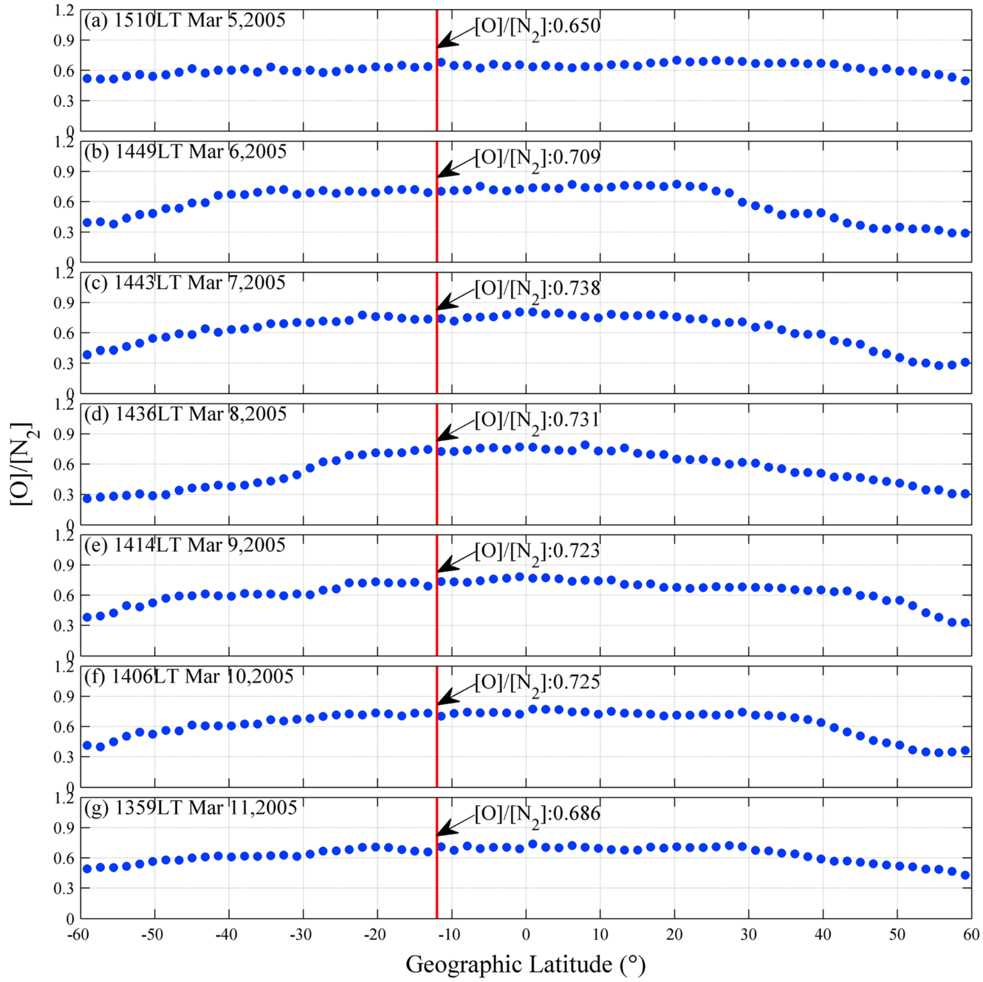

Figure 5. The variations of daytime [O]/[N_2] ratio as functions of geographic latitude (60°S–60°N) around the geographic longitude of Jicamarca (76.8°W) during the period of 5–11 March 2005. The red vertical line represents the geographic latitude of Jicamarca (12°S), and the mean values of [O]/[N_2] near the latitude are marked at the top of the red vertical line for each day.

irregularities in the *F* region during this interval. It indicates that the start time of LPSs is dominant at 21:00–03:00 LT and 08:00–14:00 LT, corresponding to the daytime and nighttime, respectively. Therefore, all the LPSs can be grouped into two categories, the daytime LPS and the nighttime LPS, in order to further discuss the LPS features. As illustrated in Figure 2 (bottom), the MPO of the geomagnetic storms has no obvious dependence on LT for all LPSs. Further work is required to give relevant theoretical explanation about this statistical feature.

3.2. Typical Daytime and Nighttime LPS Events

In order to show the complete process of a daytime LPS, we present a typical event during 5–11 March 2005. Figure 3 illustrates the variations of f_oF_2, h_mF_2, $dH_{\text{JIC-PIU}}$, *SYM-H*, IMF B_z (gray line), and *AE* index (cyan line) on 5–11 March 2005. The blue curves in Figures 3a–3c denote the 27 day running medians of these parameters. As seen from Figure 3, the *SYM-H* index drops to ~−65 nT on 6 March during this geomagnetic storm. At the same time, the IMF B_z component (Figure 3e) oscillates rapidly between northward and southward directions, and the *AE* index increases to ~1900 nT. After the onset of the geomagnetic storm, these parameters gradually return to normal values in the following days. The *AE* index tends to increase for every major southward IMF B_z interval during the storm time.

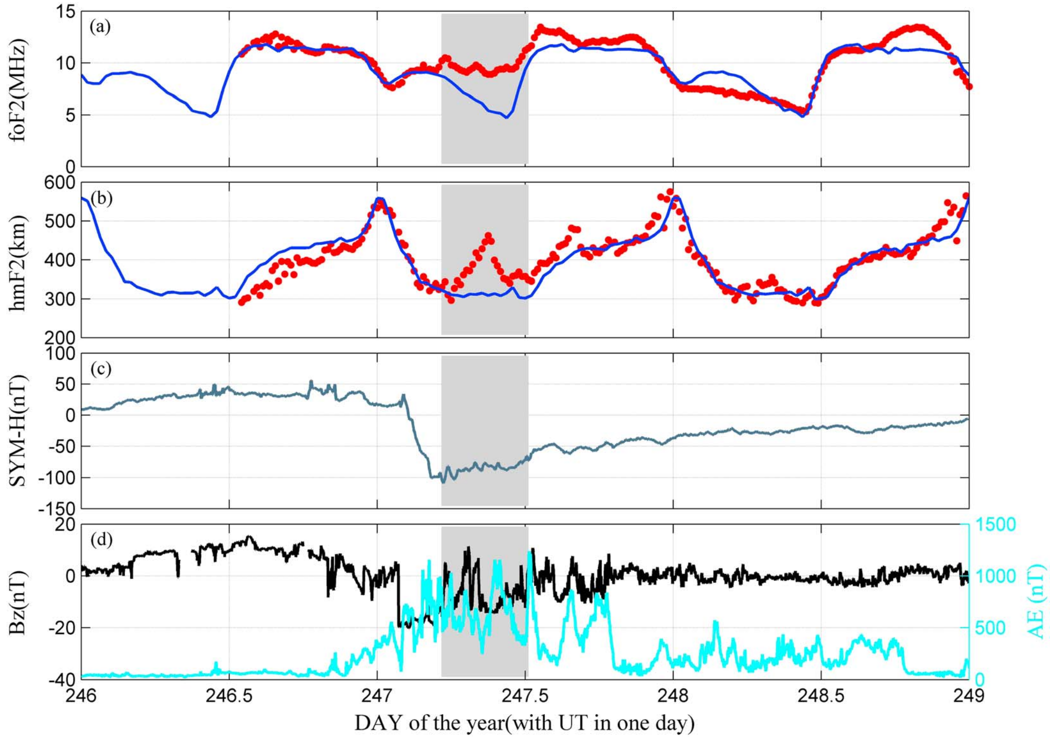

Figure 6. Variations of (a) critical frequency of F_2 layer (f_oF_2), (b) peak height of F_2 layer (h_mF_2), (c) *SYM-H*, and (d) IMF B_z (gray line) and *AE* index (cyan line) during 3–5 September 2002. The blue curves of Figures 6a and 6b denote the 27 day moving median value of these parameters. The gray shaded area gives the period of the nighttime long-duration positive storm (LPS).

The daytime LPS occurs at about 17:00 UT on 8 March and persists to 02:30 UT on 9 March during the recovery phase of this geomagnetic storm. The gray shaded area indicates the period of this daytime LPS. It is evident that the positive phase lasts for more than 9 h (Figure 3a). Meanwhile, the h_mF_2 (Figure 3b) drops by about 30–40 km. During the LPS on 8 March, the $dH_{\text{JIC-PIU}}$ has a decline phase to a minimum of −50 nT, which stands for a westward equatorial electrojet. This westward equatorial electrojet lasts about 9–10 h on 8 March. Taking into account the direction and the duration, the most likely effects here are DDEF, which is typically westward on the dayside and occurs often with a long duration [*Blanc and Richmond*, 1980; *Scherliess and Fejer*, 1997]. So the reversed westward electrojet should be attributed to a daytime westward DDEF. It is a clear phenomenon that f_oF_2 attains larger values relative to their 27 day running mean values and are in antiphase with h_mF_2 in company of the westward electric field over Jicamarca. Figure 4 (left) gives the variations of f_oF_2, h_mF_2, and $dH_{\text{JIC-PIU}}$ and Figure 4 (right) the deviations of these parameters during the LPS of 8–9 March 2005. The blue curves denote the 27 day moving median value of these parameters. The figure shows good one-to-one correspondences among counter electrojet, decreased h_mF_2, and increased f_oF_2 in the equatorial ionosphere LPS. *Zhao et al.* [2005] have mentioned similar phenomenon at Jicamarca during the October to November 2003 superstorms.

Besides the effects of westward electric field, the influence of the storm time thermospheric circulation is also verified in this event. Figure 5 displays the variations of daytime [O]/[N_2] ratio as functions of geographic latitude (60°S–60°N) around the geographic longitude of Jicamarca (76.8°W) during the period of 5–11 March 2005. The red vertical line represents the geographic latitude of Jicamarca (12°S), and the mean values of [O]/[N_2] near the latitude are marked at the top of the red vertical line for each day. The GUVI [O]/[N_2] data are taken at a relatively fixed local time 14:00–15:00 over these days. The local time 14:00–15:00 also falls within the period of the LPS on March 8, so the data of [O]/[N_2] can better reflect the altered storm time thermospheric circulation. Taking the first day (Figure 5a) as a reference of quiet time [O]/[N_2] ratio, it is observed that there is an enhancement of [O]/[N_2] ratio during the storm

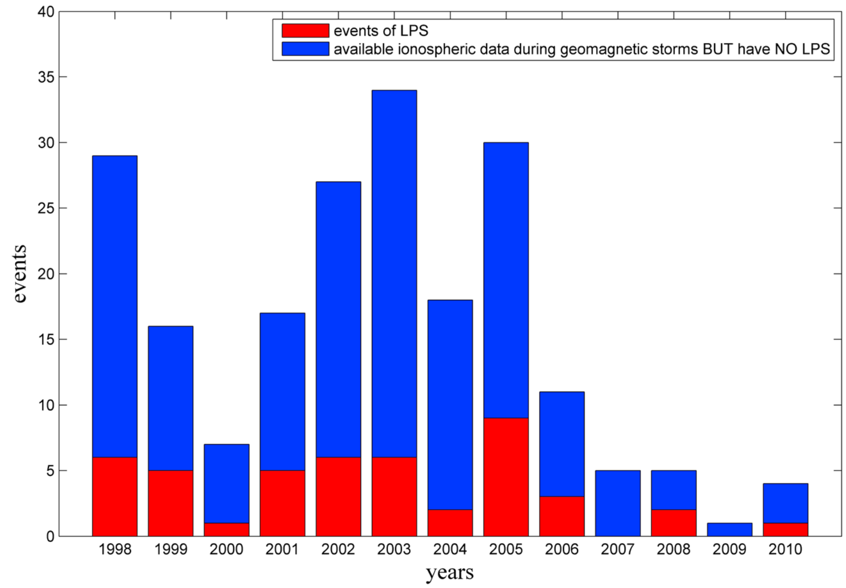

Figure 7. The yearly distribution of the geomagnetic storms in 1998–2010 when the measurements of ionosonde are available at Jicamarca. The red bars show the events of the observed long-duration positive storms (LPSs) in each year.

conditions and the LPS on March 8 over Jicamarca. But the largest absolute increment of [O]/[N_2] ratio is less than 0.1 (about 0.08) by comparing the quiet time value (Figure 5a on March 5) with the LPS value (Figure 5d on March 8). It is probable that the altered storm time thermospheric circulation is an assistant factor for the formation of this daytime LPS.

A typical nighttime LPS is also presented in Figure 6 to display the complete process during the days of year 246–248 in 2002. Figure 6 illustrates the variations of f_oF_2, h_mF_2, *SYM-H*, IMF B_z, and *AE* index during 3–5 September 2002. The blue curves in Figures 6a and 6b denote the 27 day moving median value of these parameters. Seen from the *SYM-H* index (Figure 6c), the main phase of this geomagnetic storm disturbance starts from the beginning of 4 September and then quickly drops to ~−100 nT in 3 h. At the same time, the IMF B_z component (Figure 6d) rapidly oscillates between the northward and southward directions, and the *AE* index rapidly increases to ~1200 nT. After these changes, these parameters gradually return to normal values in about 2 days.

The nighttime LPS occurs from about 5:00 UT to 12:00 UT on 4 September (from 0:00 LT to 7:00 LT on the day) during this geomagnetic storm. The gray shaded area also indicates the period of this nighttime LPS. The positive phase lasts for about 7 h from the curve of f_oF_2 (Figure 6a). Meanwhile, the h_mF_2 (Figure 6b) values also have a significant enhancement for more than 100 km. The uplifting effects are most likely caused by eastward electric fields in the region of magnetic equator. And the eastward electric fields are also probably DDEF because of the long duration and the eastward direction at night [*Blanc and Richmond*, 1980; *Scherliess and Fejer*, 1997]. As a summary, a significant uplifting of F_2 layer caused by eastward DDEF is found during this nighttime LPS over Jicamarca.

3.3. Statistics and Characteristics of the LPSs

Figure 7 gives the yearly distribution of the geomagnetic storms in 1998–2010 when the measurements of ionosonde are available at Jicamarca. The red bars show the LPS events in each year. As can be seen from Figure 7, a stable ratio of the number of LPS to total geomagnetic storm events varies between 10 and 30%, apart from the individual months that LPSs do not appear.

Figure 8 shows the monthly distribution of the geomagnetic storms and the observed LPSs in 1998–2010 at Jicamarca. Compared with Figure 7, a similar ratio is also found from Figure 8. The equinoctial months have a higher incidence. A salient feature is that the ratio of equatorial LPSs to geomagnetic storms has no obvious dependence on season and solar activity from Figures 7 and 8.

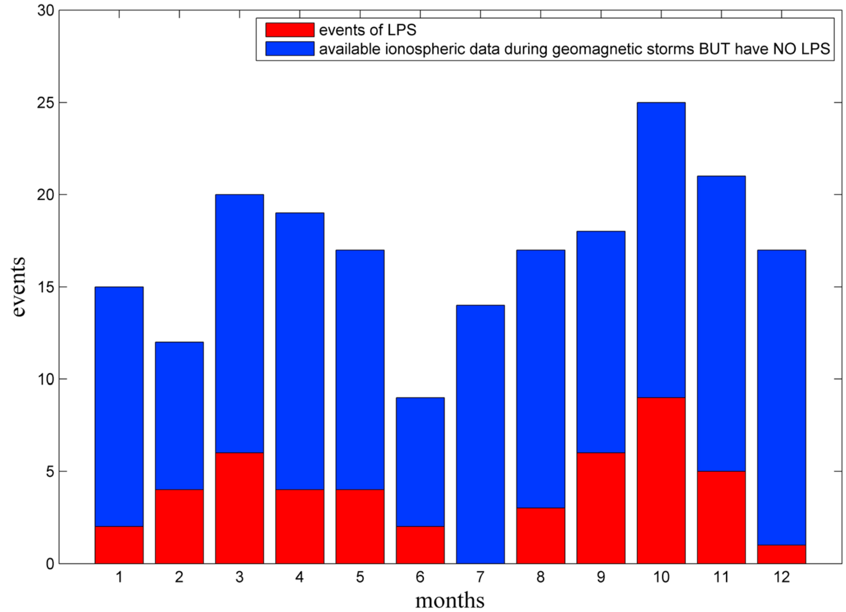

Figure 8. The monthly distribution of the geomagnetic storms and the observed long-duration positive storms in 1998–2010 when the measurements of ionosonde are available at Jicamarca. The red bars show the events of the observed long-duration positive storms (LPSs) in each month.

Huang [2013] had obtained the findings that the intensities of disturbance dynamo electric fields are highly dependent on various parameters containing solar activities and seasonal effects by using model simulations. The occurrence of LPSs during geomagnetic storms does not reflect the dependency in our statistical results in spite of the fact that the occurrence of LPSs is closely related to DDEFs. The insufficiency of the number of samples may affect the statistical features in this study.

In order to establish a connection between LPSs and geomagnetic storms, Figure 9 shows the distribution of the time lag of the onset of LPSs after the main phase of the geomagnetic storms. As depicted in Figure 9, the occurrence of the LPSs approximately exponentially decreases with time after the main phase of the geomagnetic storms, and most of the LPSs occur within 3 days. The declining residual energy makes the occurrence of the LPSs decreasing.

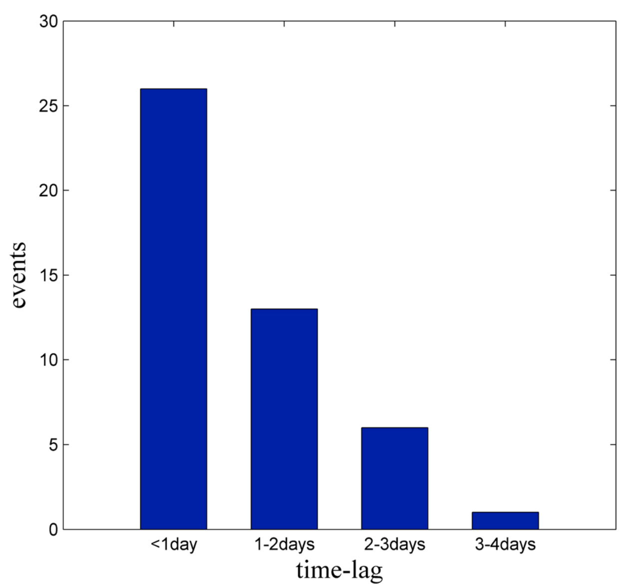

Figure 9. The distribution of the time lag of the onset of long-duration positive storms (LPSs) after the main phase of the geomagnetic storms.

4. Discussion

It is generally considered that the positive ionospheric storm effects are close to the electric fields, wind fields, and neutral composition changes at low latitude [e.g., *Danilov and Belik*, 1992; *Prölss*, 1995; *Buonanto*, 1999; *Mendillo*, 2006]. In this work, the Jicamarca station is near the magnetic equator. The F_2 layer uplifting due to vertical drift by the neutral winds can be ignored because the magnetic field lines are horizontal over Jicamarca.

In the analysis of the daytime LPS, it is obvious that the westward electric field is an important feature during LPS. The available data of $dH_{JIC\text{-}PIU}$ during all of the

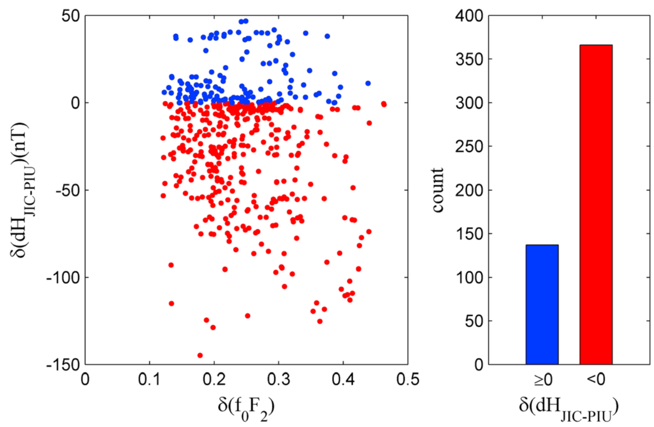

Figure 10. (left) The distribution of δ (f_oF_2) as a function of δ ($dH_{\text{JIC-PIU}}$) and (right) the distribution of counts of positive (eastward electric fields) and negative (westward electric fields) deviation of δ ($dH_{\text{JIC-PIU}}$) during the daytime long-duration positive storms (LPSs). The red dots of the figure also display the negative (westward electric fields) deviation of δ ($dH_{\text{JIC-PIU}}$).

daytime LPSs are gathered for further analysis. Figure 10 (left) gives the distribution of δ (f_oF_2) as a function of δ ($dH_{\text{JIC-PIU}}$) and Figure 10 (right) the distribution of counts of positive (eastward electric fields) and negative (westward electric fields) deviation of δ ($dH_{\text{JIC-PIU}}$). The δ (f_oF_2) values use the relative deviation (=($f_oF_2 - (f_oF_2)_Q$)/$(f_oF_2)_Q$; $(f_oF_2)_Q$ is the 27 day sliding smooth median value), while the δ ($dH_{\text{JIC-PIU}}$) values use the absolute deviation (=($dH_{\text{JIC-PIU}} - (dH_{\text{JIC-PIU}})_Q$), and $(dH_{\text{JIC-PIU}})_Q$ is the 27 day sliding smooth median value) because the $(dH_{\text{JIC-PIU}})_Q$ values are oscillating frequently between positive and negative. Figure 10 shows that the counter westward electric field effects are very significant during all of the daytime LPSs. Based on this counter westward electric field and the decreased height of F_2 layer, it is possible to infer that the pull-down effect to the F region caused by the counter westward electric field under the action of $E \times B$ vertical drift makes the two equatorial anomaly crests converge to the equatorial regions and the plasmas gather toward the equator along the magnetic field lines and finally causes the significant positive ionospheric storm effects. And these processes are consistent with the results reported by *Basu et al.* [2009] and *Liu et al.* [2012a], in which daytime equatorial ionization anomaly (EIA) structure collapses in the presence of counter electrojet and simultaneous electron density enhancements over the EIA trough region. *Pedatella et al.* [2009] emphasized the importance of the enhanced eastward electric field in the generation of LPS effects, and the difference in the direction of the electric field also reflects the particularity of the equatorial regions compared to the low latitudes and midlatitudes. The enhanced eastward electric field could produce the negative ionospheric storm effects in the equatorial regions because of the opposite processes of the above daytime LPSs.

The effects of the storm time thermospheric circulation are also verified in this work using the data of [O]/[N_2] ratio from TIMED/GUVI during the daytime LPSs. As shown in the previous part and the Appendix A, a weak enhancement of [O]/[N_2] ratio is observed during the period of the daytime LPSs over Jicamarca. The effects of neutral composition changes are much weaker as compared to the impacts of electric fields in the daytime LPSs over Jicamarca. The conclusion resembles the simulation results reported by *Lin et al.* [2005], in which the composition effects do not produce a density increase as large as that produced by electric field and wind field effects.

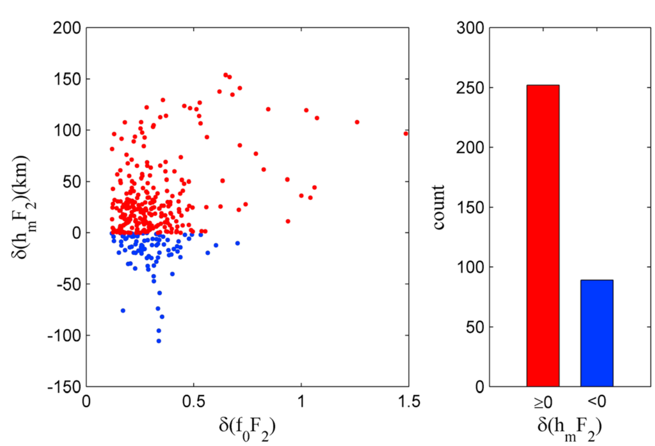

Figure 11. (left) The distribution of δ (f_oF_2) as a function of δ (h_mF_2) and (right) the distribution of counts of positive and negative deviations of δ (h_mF_2) during the nighttime long-duration positive storms (LPSs). The red dots of the figure also show the positive deviation of δ (h_mF_2).

At night, the effects of electric fields are probably the decisive factor for the nighttime LPS over Jicamarca. The value of h_mF_2 has a significant increase during the period of nighttime LPSs. And the phenomenon is also apparent in the previous event and the supplementary case in the Appendix A. Similar to Figure 10, Figure 11 (left) displays the

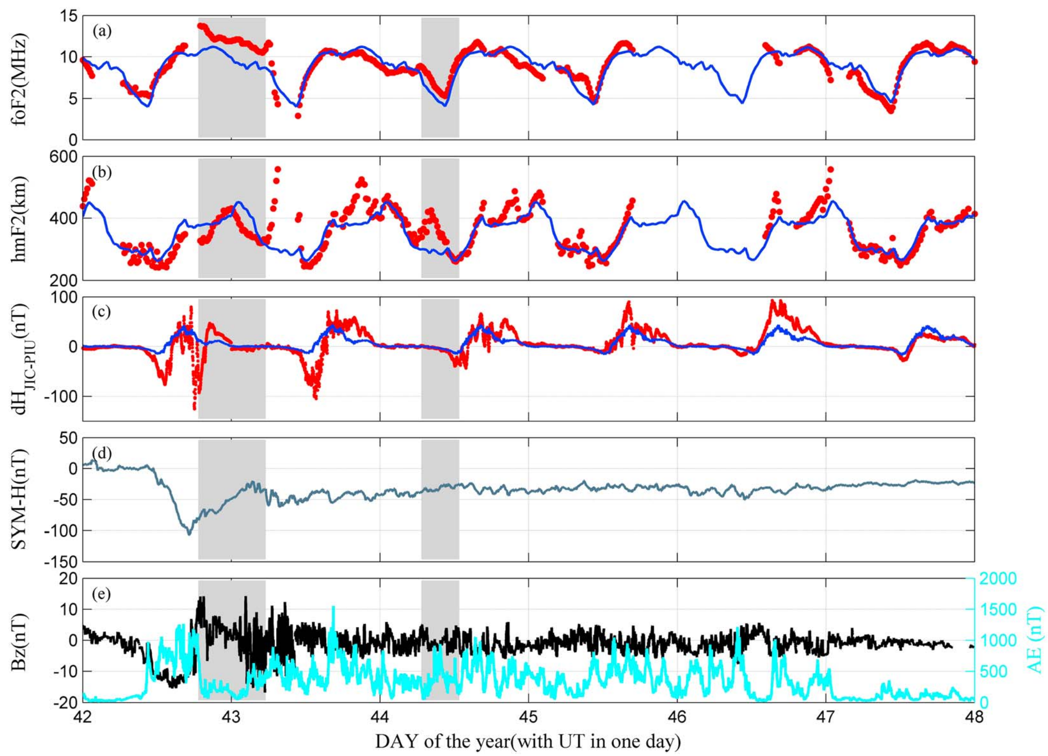

Figure A1. Similar to Figure 3 but during 11–16 February 2004. The gray shaded areas indicate the period of a daytime long-duration positive storm (LPS) and a nighttime LPS.

nighttime distribution of δ (f_oF_2) as a function of δ (h_mF_2) and Figure 11 (right) the distribution of counts of positive and negative deviation of δ (h_mF_2). The δ (f_oF_2) values are also the relative deviation (=($f_oF_2-(f_oF_2)_Q)/(f_oF_2)_Q$; $(f_oF_2)_Q$ is the 27 day sliding smooth median value), and the δ (h_mF_2) values are the absolute deviation (=($h_mF_2-(h_mF_2)_Q$); $(h_mF_2)_Q$ is the 27 day sliding smooth median value). A significant positive phase of δ (h_mF_2) can be observed from the figure. A nighttime eastward electric field can lift plasma upward due to the $E\times B$ vertical drift so that the F_2 layer comes to a higher altitude. As previously mentioned, the action is most likely caused by DDEF because of the eastward direction and the long duration during the nighttime LPSs [*Blanc and Richmond*, 1980; *Scherliess and Fejer*, 1997]. With the risen height of F_2 layer, more plasmas are available at higher altitudes, where the recombination rates are low so that the electron densities are increased. Relative to the daytime cases, the height of F_2 layer must be increased more significantly to get the effects of ionospheric positive storms, because the effects of solar ionization are disappear at night. The processes give a better explanation of the content in Figure 11.

Although this work gives some observational characteristics and theoretical explanations for the LPSs over Jicamarca, many aspects of the phenomenon are still not well understood. The ionospheric storm is a complex process, and every storm has its unique feature. Therefore, more observations and numerical simulations are required to do more detailed research for the LPS effects, as earlier suggested by *Buonsanto* [1999].

5. Conclusion

In this work, we conducted a statistical analysis to investigate the LPS effects at Jicamarca in the equatorial regions. We collected the ionogram data recorded at Jicamarca during the geomagnetic storms in 1998–2010 to find LPSs using the criterion that the storm time relative deviation of N_mF_2 exceeds 25% for more than 6 h. We obtained the statistical characteristics and analyzed the typical

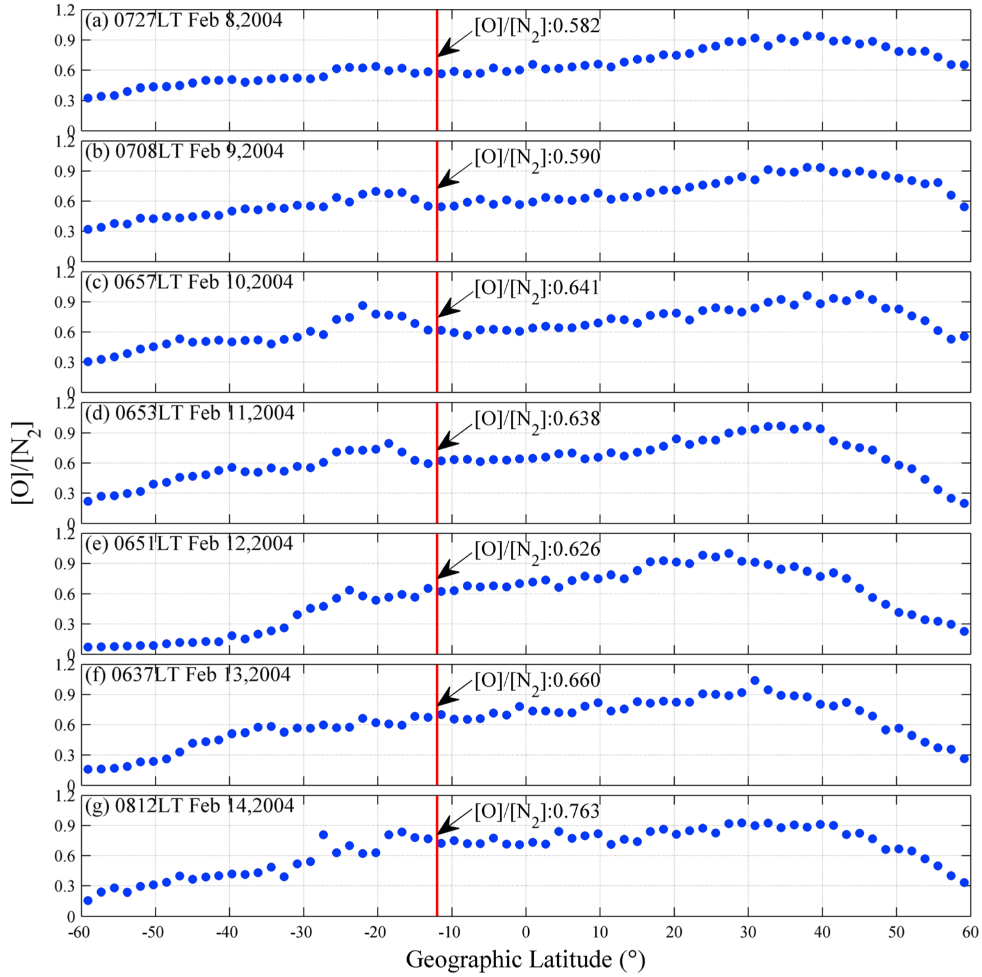

Figure A2. Similar to Figure 5 but during the period of 8–14 February 2004.

case of daytime LPS and nighttime LPS and then discussed the possible mechanisms. The major conclusions are summarized as follows:

1. In total, 46 LPSs are found during the 204 available geomagnetic storms of 250 geomagnetic storms in 1998–2010 over Jicamarca. From the statistical results, the ratio of equatorial LPSs to geomagnetic storms has no obvious dependence on season and solar activity.
2. The occurrence of the LPSs approximately exponentially decreases with time after the main phase of the geomagnetic storms, and most of the LPSs occur within 3 days. This phenomenon is probably related to the energy dissipation of the geomagnetic storms.
3. The westward electrojet is a very significant feature during the daytime LPSs, while the changing of neutral composition is weak. The h_mF_2 values have a significant enhancement during the nighttime LPSs.
4. About the process and mechanism of the daytime LPSs, it is possible to infer that the pull-down effect to the F region caused by the counter westward electric field under the action of $E \times B$ vertical drift makes the two equatorial anomaly crests converge to the equatorial regions and the plasmas gather toward the equator along the magnetic field lines and finally causes the significant daytime LPS effects. The altered storm time thermospheric circulation may be an assistant factor for the formation of the daytime LPSs. For the nighttime LPSs, the significant enhancement of h_mF_2 makes more plasma available at higher altitudes, where the recombination rates are low so that the electron densities are increased.

Appendix A: Another Event Example

Figure A1 illustrates the variations of f_oF_2, h_mF_2, $dH_{\text{JIC-PIU}}$, *SYM-H*, IMF B_z (gray line), and *AE* index (cyan line) during 11–16 February 2004. The blue curves of Figures A1a–A1c denote the 27 day moving median value of these parameters.

During the geomagnetic storm, the minimum value of *SYM-H* index reaches −100 nT. Both a daytime LPS (about from 19:00 UT on 11 February to 05:30 UT on 12 February) and a nighttime LPS (about from 06:45 UT on 13 February to 12:45 UT on 13 February) occur during the storm time. The gray shaded areas give the period of the two LPSs.

This event shows consistent features as previous events. The reversed westward electrojet and the decreased h_mF_2 appear during the daytime LPS. The phenomenon of the increased h_mF_2 is significant during the nighttime LPS.

Similar to Figure 9, Figure A2 displays the variations of daytime [O]/[N_2] ratio but during the period of 8–14 February 2004. The data before 10 February can be used as a reference quiet time [O]/[N_2] ratio. There may be some deviations because the local time of the [O]/[N_2] data and the daytime LPS are not exactly the same. But a weak enhancement of [O]/[N_2] ratio is also observed during the period of the daytime LPS.

Acknowledgments
The *Dst* index is obtained from the World Data Center for Geomagnetism, Kyoto (http://wdc.kugi.kyoto-u.ac.jp/dstdir/index.html). The Omni data are obtained from the GSFC/SPDF OmniWeb interface at http://omniweb.gsfc.nasa.gov. We are grateful to B.W. Reinisch of the Center for Atmospheric Research, University of Massachusetts Lowell, for providing the ionogram data of DIDBase. The data of [O]/[N_2] ratio are obtained from TIMED/GUVI (http://guvi.jhuapl.edu/). This research was supported by National Natural Science Foundation of China (41231065), the Chinese Academy of Sciences project (KZZD-EW-01-3), National Key Basic Research Program of China (2012CB825604), and National Natural Science Foundation of China (41174137 and 41321003).

Alan Rodger thanks Alexander Namgaladze and another reviewer for their assistance in evaluating this paper.

References

Abdu, M. A. (1997), Major phenomena of the equatorial ionospherethermosphere system under disturbed conditions, *J. Atmos. Sol. Terr. Phys.*, *59*, 1505–1519.
Anderson, D., A. Anghel, K. Yumoto, M. Ishitsuka, and E. Kudeki (2002), Estimating daytime vertical *E*×*B* drift velocities in the equatorial *F* region using ground-based magnetometer observations, *Geophys. Res. Lett.*, *29*(12), 1596, doi:10.1029/2001GL014562.
Bagiya, M. S., K. N. Iyer, H. P. Joshi, S. V. Thampi, T. Tsugawa, S. Ravindran, R. Sridharan, and B. M. Pathan (2011), Low-latitude ionospheric-thermospheric response to storm time electrodynamical coupling between high and low latitudes, *J. Geophys. Res.*, *116*, A01303, doi:10.1029/2010JA015845.
Bagiya, M. S., R. Hazarika, F. I. Laskar, S. Sunda, S. Gurubaran, D. Chakrabarty, P. K. Bhuyan, R. Sridharan, B. Veenadhari, and D. Pallamraju (2014), Effects of prolonged southward interplanetary magnetic field on low-latitude ionospheric electron density, *J. Geophys. Res. Space Physics*, *119*, 5764–5776, doi:10.1002/2014JA020156.
Basu, S., S. Basu, J. Huba, J. Krall, S. E. McDonald, J. J. Makela, E. S. Miller, S. Ray, and K. Groves (2009), Day-to-day variability of the equatorial ionization anomaly and scintillations at dusk observed by GUVI and modeling by SAMI3, *J. Geophys. Res.*, *114*, A04302, doi:10.1029/2008JA013899.
Blanc, M., and A. D. Richmond (1980), The ionospheric disturbance dynamo, *J. Geophys. Res.*, *85*, 1669–1686, doi:10.1029/JA085iA04p01669.
Buonsanto, M. J. (1999), Ionospheric storm: A review, *Space Sci. Rev.*, *88*, 563–601.
Burns, A. G., S. C. Solomon, W. Wang, and T. L. Killeen (2007), The ionospheric and thermospheric response to CMEs: Challenges and successes, *J. Atmos. Sol. Terr. Phys.*, *69*, 77–85.
Chen, Y., L. Liu, and W. Wan (2012), The discrepancy in solar EUV-proxy correlations on solar cycle and solar rotation timescales and its manifestation in the ionosphere, *J. Geophys. Res.*, *117*, A03313, doi:10.1029/2011JA017224.
Danilov, A. D. (2013), Ionospheric *F*-region response to geomagnetic disturbances, *Adv. Space Res.*, *52*, 343–366.
Danilov, A. D., and L. D. Belik (1992), Thermosphere composition and the positive phase of an ionospheric storm, *Adv. Space Res.*, *12*, 257–260.
Danilov, A. D., and J. Lăstovička (2001), Effects of geomagnetic storms on the ionosphere and atmosphere, *Int. J. Geomagn. Aeron.*, *2*, 209–224.
Fejer, B. G. (1986), Equatorial ionospheric electric fields associated with magnetospheric disturbances, in *Solar Wind Magnetosphere Coupling*, edited by Y. Kamide and J. A. Slavin, pp. 519–545, Terra Sci., Tokyo.
Fejer, B. G. (1997), The electrodynamics of the low-latitude ionosphere: Recent results and future challenges, *J. Atmos. Sol. Terr. Phys.*, *59*, 1465–1482, doi:10.1016/S1364-6826(96)00149-6.
Fejer, B. G., M. F. Larsen, and D. T. Farley (1983), Equatorial disturbance dynamo electric fields, *Geophys. Res. Lett.*, *10*, 537–540, doi:10.1029/GL010i007p00537.
Fuller-Rowell, T. J., M. V. Codrescu, H. Rishbeth, R. J. Moffett, and S. Quegan (1996), On the seasonal response of the thermosphere and ionosphere to the geomagnetic storms, *J. Geophys. Res.*, *101*, 2343–2353, doi:10.1029/95JA01614.
Huang, C. M. (2013), Disturbance dynamo electric fields in response to geomagnetic storms occurring at different universal times, *J. Geophys. Res. Space Physics*, *118*, 496–501, doi:10.1029/2012JA018118.
Huang, X., and B. W. Reinisch (1996), Vertical electron density profile from the Digisonde network, *Adv. Space Res.*, *18*, 121–129, doi:10.1016/0273-1177(95)00912-4.
Huang, C.-S., J. C. Foster, L. P. Goncharenko, P. J. Erickson, W. Rideout, and A. J. Coster (2005a), A strong positive phase of ionospheric storms observed by the Millstone Hill incoherent scatter radar and global GPS network, *J. Geophys. Res.*, *110*, A06303, doi:10.1029/2004JA010865.
Huang, C.-S., J. C. Foster, and M. C. Kelley (2005b), Long-duration penetration of the interplanetary electric field to the low-latitude ionosphere during the main phase of magnetic storms, *J. Geophys. Res.*, *110*, A11309, doi:10.1029/2005JA011202.
King, J. H., and N. E. Papitashvili (2005), Solar wind spatial scales in and comparisons of hourly Wind and ACE plasma and magnetic field data, *J. Geophys. Res.*, *110*, A02104, doi:10.1029/2004JA010649.
Lemaire, J. F., and K. I. Gringauz (1998), *The Earth's Plasmasphere*, Cambridge Univ. Press, New York.
Lin, C. H., A. D. Richmond, R. A. Heelis, G. J. Bailey, G. Lu, J. Y. Liu, H. C. Yeh, and S.-Y. Su (2005), Theoretical study of the low- and midlatitude ionospheric electron density enhancement during the October 2003 superstorm: Relative importance of the neutral wind and the electric field, *J. Geophys. Res.*, *110*, A12312, doi:10.1029/2005JA011304.

Liu, J., B. Zhao, and L. Liu (2010), Time delay and duration of ionospheric total electron content responses to geomagnetic disturbances, *Ann. Geophys.*, *28*, 795–805, doi:10.5194/angeo-28-795-2010.
Liu, J., L. Liu, B. Zhao, Y. Wei, L. Hu, and B. Xiong (2012a), High-speed stream impacts on the equatorial ionization anomaly region during the deep solar minimum year 2008, *J. Geophys. Res.*, *117*, A10304, doi:10.1029/2012JA018015.
Liu, J., L. Liu, B. Zhao, J. Lei, J. P. Thayer, and R. L. McPherron (2012b), Superposed epoch analyses of thermospheric response to CIRs: Solar cycle and seasonal dependencies, *J. Geophys. Res.*, *117*, A00L10, doi:10.1029/2011JA017315.
Liu, L., W. Wan, C. C. Lee, B. Ning, and J. Y. Liu (2004), The low latitude ionospheric effects of the April 2000 magnetic storm near the longitude 120°E, *Earth Planets Space*, *56*, 607–612.
Mednikova, N. B. (1957), Mid-latitude ionospheric disturbances, in *Physics of Solar Corpuscular Fluxes and Their Impact on the Upper Atmosphere of the Earth* [in Russian], p. 183, Acad. Press of USSR, Moscow.
Mendillo, M. (2006), Storms in the ionosphere: Patterns and processes for total electron content, *Rev. Geophys.*, *44*, RG4001, doi:10.1029/2005RG000193.
Ngwira, C. M., L.-A. McKinnell, P. J. Cilliers, and A. J. Coster (2012), Ionospheric observations during the geomagnetic storm events on 24–27 July 2004: Long-duration positive storm effects, *J. Geophys. Res.*, *117*, A00L02, doi:10.1029/2011JA016990.
Pedatella, N. M., J. Lei, K. M. Larson, and J. M. Forbes (2009), Observations of the ionospheric response to the 15 December 2006 geomagnetic storm: Long-duration positive storm effect, *J. Geophys. Res.*, *114*, A12313, doi:10.1029/2009JA014568.
Prölss, G. W. (1995), Ionospheric *F* region storms, in *Handbook of Atmospheric Electrodynamics*, vol. 2, edited by H. Volland, pp. 195–248, CRC Press, Boca Ration, Fla.
Sastri, J. H. (1988), Equatorial electric fields of ionospheric disturbance dynamo origin, *Ann. Geophys.*, *6*, 635–642.
Sastri, J. H., N. Jyoti, V. V. Somayajulu, H. Chandra, and C. V. Devasia (2000), Ionospheric storm of early November 1993 in the Indian equatorial region, *J. Geophys. Res.*, *105*, 18,443–18,455, doi:10.1029/1999JA000372.
Scherliess, L., and B. G. Fejer (1997), Storm time dependence of equatorial disturbance dynamo zonal electric fields, *J. Geophys. Res.*, *102*, 24,037–24,046, doi:10.1029/97JA02165.
Schunk, R. W., and A. F. Nagy (2000), *Ionospheres: Physics, Plasma Physics, and Chemistry*, Cambridge Univ. Press, New York.
Strickland, D. J., R. R. Meier, R. L. Walterscheid, J. D. Craven, A. B. Christensen, L. J. Paxton, D. Morrison, and G. Crowley (2004), Quiet-time seasonal behavior of the thermosphere seen in the far ultraviolet dayglow, *J. Geophys. Res.*, *109*, A01302, doi:10.1029/2003JA010220.
Vijaya Lekshmi, D., N. Balan, S. Tulasi Ram, and J. Y. Liu (2011), Statistics of geomagnetic storms and ionospheric storms at low and midlatitudes in two solar cycles, *J. Geophys. Res.*, *116*, A11328, doi:10.1029/2011JA017042.
Wanliss, J. A., and K. M. Showalter (2006), High-resolution global storm index: *Dst* versus *SYM-H*, *J. Geophys. Res.*, *111*, A02202, doi:10.1029/2005JA011034.
Wei, Y., W. Wan, Z. Pu, M. Hong, Q. Zong, J. Guo, B. Zhao, and Z. Ren (2011), The transition to overshielding after sharp and gradual interplanetary magnetic field northward turning, *J. Geophys. Res.*, *116*, A01211, doi:10.1029/2010JA015985.
Zhao, B., W. Wan, and L. Liu (2005), Responses of equatorial anomaly to the October–November 2003 superstorms, *Ann. Geophys.*, *23*, 693–706, doi:10.5194/angeo-23-693-2005.

